Feedback Control for Electromagnetic Vibration Feeder*

(Applications of Two-Degrees-of-Freedom Proportional plus Integral plus Derivative Controller with Nonlinear Element)

Tomoharu DOI**, Koji YOSHIDA***,
Yutaka TAMAI****, Katsuaki KONO****,
Kazufumi NAITO**** and Toshiro ONO*****

An electromagnetic-type vibratory feeder of is a typical transportation device used in automatic weighers. As existing feeders are driven by feedforward control, the so-called "firing angle control", the driver cannot negate sudden disturbances. In this study, we consider applying a feedback control for such a feeder system. First, we give the two details of modelings for the vibration part and for the electromagnetic force part. Next, a feedback control system is constructed for the electromagnetic vibration feeder for which we propose a two-degrees-of-freedom proportional plus integral plus derivative (PID) controller with nonlinear elements. Next, we apply the feedback control to the feeder with a standard trough. Finally, we consider a method compatible with many varieties of troughs by adjusting a nonlinear element. On the basis of the results of some experiments, we confirm that the two-degrees-of-freedom PID control is more effective than the conventional firing angle control.

Key Words: Vibration Control, Feeding Drive, Nonlinear Control, Electromagnetic Actuator, Two-Degrees-of-Freedom PID Control, Modeling

1. Introduction

For stuff-bagging processes of various food manufacturing industries, an automatic weigher is a very important device. Automatic weighers were developed in 1973, and have subsequently been improved to become highly accurate and effective. The electromagnetic vibration feeder considered in this paper is an important transportation device which transports the material supplied to the weighing unit systematically. However, after the firing angle control (feedforward control) was applied to the feeder, further improvement has not been carried out up to the present.

In this study, a feedback control system is constructed for the electromagnetic vibration feeder for which we propose a two-degrees-of-freedom proportional plus integral plus derivative (PID) controller with nonlinear elements. First, we give the details of modelings for the vibration part and the electromagnetic force part. Next, we apply the feedback control to the feeder with a standard trough. Then, we consider a method compatible with a variety of troughs by adjusting a nonlinear element of the two-degrees-of-freedom PID controller. On the basis of the results of some experiments, we confirm that the two-degrees-of-freedom PID control is more effective than the firing angle control.

* Received 8th March, 2000. Japanese original: Trans. Jpn. Soc. Mech. Eng., Vol. 65, No. 635, C (1999), pp. 2651-2658 (Received 3rd April, 1998)

** Department of Systems and Control Engineering, Faculty of Engineering, Osaka Prefectural College of Technology, 26-12 Saiwai-cho, Neyagawa, Osaka 572-8572, Japan. E-mail: doi@sys.osaka-pct.ac.jp

*** Department of System Engineering, Faculty of Computer Science and System Engineering, Okayama Prefectural University, 111 Kuboki, Soja, Okayama 719-1197, Japan

**** Research & Development Department, Ishida Co., Ltd., 959-1 Shimomagari, Ritto-cho, Kurita-gun, Shiga 520-3026, Japan

***** Department of Mechanical Systems Engineering, College of Engineering, Osaka Prefecture University, 1-1 Gakuen-cho, Sakai, Osaka 599-8531, Japan

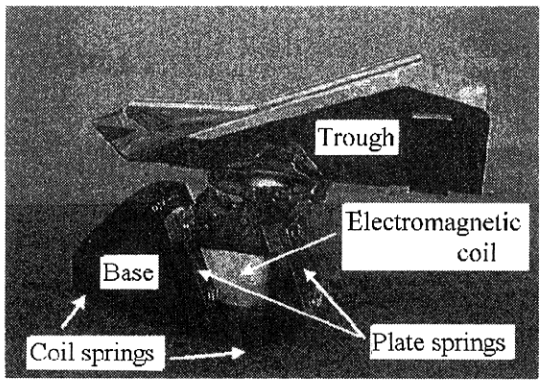

Fig. 1 Electromagnetic-type vibratory feeder

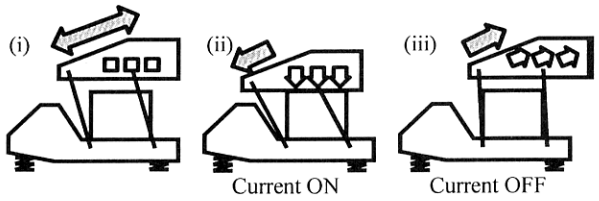

Fig. 2 Process of the transportation

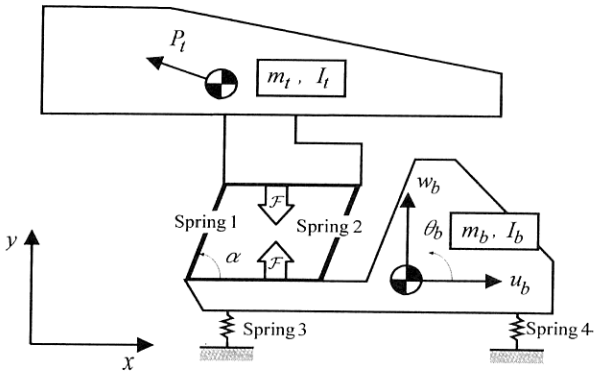

Fig. 3 Model of the vibratory element

Table 1 Nomenclatures used in the modeling

	Coordinate axes
x	Horizontal absolute coordinate axis
y	Vertical absolute coordinate axis
θ	Rotary absolute coordinate axis
P	Movable direction of plate springs
	Relative coordinate axis for base
	Variables
P_t	Displacement for P axis of trough
u_b	Displacement for x axis of base
w_b	Displacement for y axis of base
θ_b	Rotate angle θ axis of base
$\mathcal{F}$	Electromagnetic force
	Parameters at a stand
m_t, m_b	Mass of trough/base
I_t, I_b	Inertia of trough/base at center of gravity
x_t, y_t	Center of gravity for x/y axis of trough
x_b, y_b	Center of gravity for x/y axis of base
x_3, y_3	Fixed point for x/y axis of spring 3
x_4, y_4	Fixed point for x/y axis of sring 4
k_1, k_2	Spring constant for P axis of spring 1/ spring 2
k_{3x}, k_{3y}	Spring constant for x/y axis of spring 3
k_{4x}, k_{4y}	Spring constant for x/y axis of spring 4
α	Angle of the plate spring
a, b	Tuning parameters for coefficient of dumping

2. Electromagnetic Vibratory Feeder

2.1 Outline of the feeder and its transportation principle

Figure 1 shows the picture of a feeder. The term "trough" refers to a plate in the shape of a conduit, for transportation. The trough can be easily changed to match the transported objects. The trough is supported by parallel plate springs and an electromagnetic coil is located under the trough. The plate springs and coil are fixed to the base. The base is supported by three coil springs. All the parts, except the trough, are called 'feeder parts' and the set of all parts, including the trough, is called the 'Feeder.'

The trough is connected to the base by plate springs, thus this system is basically equivalent to a mass-spring system with a resonance frequency ω. The feeder is in resonance if it is driven at the resonance frequency ω. The resonance phenomenon is highly efficient because significant displacement is caused as output by a small amount of power as input.

Figure 2 shows a transportation process of transported objects. The shaded arrow indicates the movable direction of the trough in resonance. Figure 2(i) demonstrates the feeder is to be in an equilibrium position. Initially, when the current flows to the electromagnet coil (hereafter termed 'Coil'), the trough is displaced to the left lower direction (see gray arrow) by electromagnetic force, as shown in Fig. 2(ii). During this time, the transported objects on the trough move in the direction of gravity (see white arrow). When the current is turned off, the plate springs and trough propel the transported objects to the upper right direction (see gray arrow), as shown in Fig. 2(iii). In this manner, the transported objects are transported forward slowly. The feeder cyclically repeats steps (ii) and (iii) shown in Fig. 2 at a resonance frequency ω.

2.2 Modeling of vibratory mechanical element

Figure 3 shows a model of the vibratory element for the feeder. Nomenclatures of coordinate axes, variables and parameters used in this modeling are listed in Table 1. A key point of this modeling is that the movable direction P of the trough is fixed by a restrictive condition. Then, the following linear dynamic model of the fourth order can be derived as the detailed model of the vibration.

$$M\ddot{Z}+C\dot{Z}+KZ=\bar{\mathcal{F}} \quad (1)$$

$$Z=[P_t \quad u_b \quad w_b \quad \theta_b]^T$$

M, K are symmetric matrices (symbol * shows the symmetry element) as follows:

$$M=\begin{bmatrix} m_t & -m_t\sin\alpha & m_t\cos\alpha & m_t\{(x_t-x_b)\cos\alpha+(y_t-y_b)\sin\alpha\} \\ * & m_t+m_b & 0 & -m_t(y_t-y_b) \\ * & 0 & m_t+m_b & m_t(x_t-x_b) \\ * & * & * & I_b+I_t+m_t\{(x_t-x_b)^2+(y_t-y_b)^2\} \end{bmatrix}$$

$$K=\begin{bmatrix} k_1+k_2 & 0 & 0 & 0 \\ 0 & k_{3x}+k_{4x} & 0 & -k_{3x}(y_3-y_b)-k_{4x}(y_4-y_b) \\ 0 & 0 & k_{3x}+k_{4x} & k_{3y}(x_3-x_b)+k_{4y}(x_4-x_b) \\ 0 & * & * & k_{3x}(y_3-y_b)^2+k_{4x}(y_4-y_b)^2+k_{3y}(x_3-x_b)^2+k_{4y}(x_4-x_b)^2 \end{bmatrix}$$

$$C=aM+bK, \quad \bar{\mathcal{F}}=[-\mathcal{F}\cos\alpha \quad 0 \quad 0 \quad 0]^T$$

Therefore this model (1) is useful to design the vibration element. The eigenfrequency from this model (1) corresponds to the results of experimental modal analysis.

The spring element of the feeder is composed of several plate springs. This model does not consider the nonlinear characteristic of the spring element[1),2)], that changes the resonance frequency in accordance with the amplitude change in resonance.

2.3 Electromagnetic actuating element

We apply the modeling technique of an electromagnetic suspension system[3] shown in Fig. 4 to this modeling. In Fig. 4, e, i, and R denote coil voltage, coil current and coil resistance, respectively. Inductance in gap z between the coil and the trough is expressed by the function $L(z)=Q(Z_\infty+z)^{-1}+L_\infty$. As a result, the electromagnetic force $\mathcal{F}$ can be expressed by

$$\mathcal{F}=\frac{1}{2}i^2\frac{\partial L(z)}{\partial z}. \qquad (2)$$

The relationship between the coil voltage and the current is expressed as

$$e=Ri+\frac{d}{dt}\{L(z)i\}, \qquad (3)$$

where Q, Z_∞ and L_∞ are constants determined by the coil. A simulation of the feeder can be constructed on a computer using Eqs. (1), (2) and (3). Moreover, a state space model[4] can be derived by the linearization of Eqs. (1), (2), and (3).

3. Structure of a Control Experiment System

3.1 Structure of feedback system

Figure 5 shows the structure of the feedback system. The manipulated variable (hereafter termed 'Amplitude Power' AP which implies 'strength of amplitude' and is dimensionless) of this feedback system is a variable of the existing firing angle control (hereafter termed 'FAC'; its details are given later). The measured variable, the controlled variable, and the command variable are assumed to be amplitudes (hereafter termed 'Gap amplitude' G_{amp}) with gap z between the trough and the surface of the coil. The part that consists of the FAC, actuator system, and vibratory element is considered a controlled system. Figure 5 shows a structure to achieve disturbance cancellation and to improve the tracking characteristic of the command variable by two-degrees-of-freedom PID controller. This structure becomes a built-in structure of the existing FAC system, which describes the two-degrees-of-freedom PID controller in general[5),6)]. Accordingly, if the manipulated variable u_{FB} shown in Fig. 5 is shut down when the system becomes unstable by the feedback controller, this structure will correspond to the present conventional system. Hence this structure becomes a fail-safe system.

3.2 Feeder and trough used in the experiment

Figure 6 shows the set up of the experimental system. This experimental feeder can transport about 10 kg maximum mass, however a feeder is usually driven by about 0.1 kg. The resonance frequency f of this feeder is 40 Hz. When the feeder transports the maximum mass, the resonance frequency changes by about 4%. However, because it is rare to transport

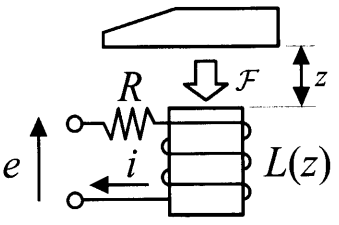

Fig. 4 Model of the electromagnetic coil

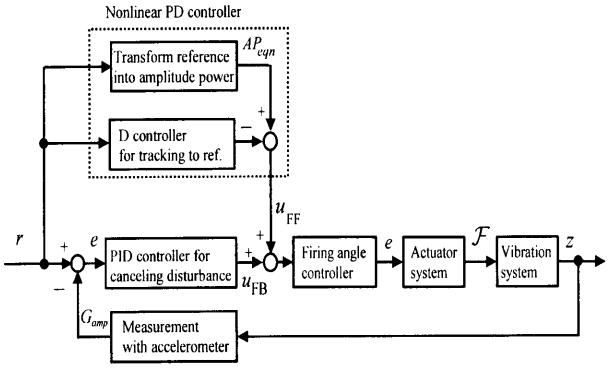

Fig. 5 Structure of the feedback system

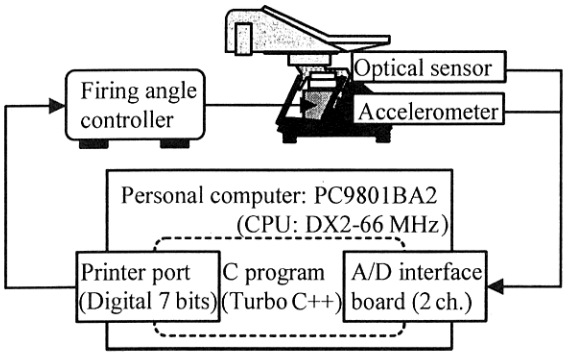

Fig. 6 Experimental system

0.5 kg or more, we neglect the change of resonance frequency caused by the change in mass of the transported objects.

Regarding the shape and type of trough, there are more than 100 varieties of troughs depending on the transported objects. For our experiment, five special kinds of troughs are used. The parameters of these troughs are listed in Table 2, and the shapes are given in Fig. 7. In the following, trough B is called the 'standard trough.' Since the mass of trough E is large, we change the combination of the plate spring elements such that the resonance frequency of the feeder becomes 40 Hz.

3.3 Feeder drive part

The FAC is used for driving an existing feeder system. Figure 8 shows the outline of the operation for FAC. The waves of Fig. 8 indicate the AC source, coil voltage and coil current, respectively. The FAC is a repetitive control method, using the crossing time (ZAT : Zero Across Time) of AC source. After the delay time L from ZAT, conducting the current into the coil is carried out. L is obtained from ΔT (constant) and AP (manipulated variable) by the following function :

$$L=F_L(\Delta T, AP) \qquad (4)$$

where ΔT (constant) is the period of the AC source. The delay time L with function F_L becomes shorter when AP becomes larger. The FAC operates based on this delay time as follows : (i) The voltage of the AC source is excited directly to the coil after the delay time L and the coil current is caused. (ii) After the peak, the coil current starts decreasing. (iii) When the coil current becomes 0 A, the AC source is turned off. Nonlinear processing like these cases (i) -(iii) are executed repeatedly with the resonance period. In the FAC, the coil current increases by AP and becomes large as a result of which vibration amplitude becomes large. The AP determines the input power for one resonance period. The resonance period corresponds to the update period of the manipulated variable. Therefore, sampling time Δt in the control experiment becomes 0.025 sec. The AP, which depends on the hardware of the FAC driver, takes the integer value from 0 to 127 (7 bits).

Table 2 Properties of the troughs

ID	Designation of the trough	Mass m_t [kg]	Inertia I_t [kgm^2]	Resonance freq. ω [rad/s]
A	Sausage	1.94	2.12×10^{-2}	40.6
B	Standard	2.01	1.98×10^{-2}	39.8
C	Boiled crab paste	2.09	2.04×10^{-2}	40.0
D	Increased in height	2.16	2.70×10^{-2}	39.9
E	Bean sprout	2.53	3.46×10^{-2}	39.8

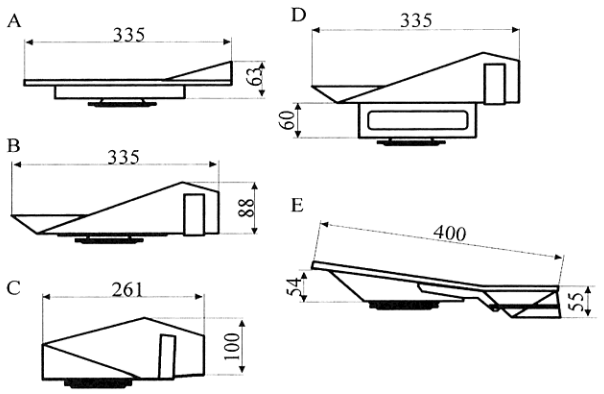

Fig. 7 Shapes of the troughs

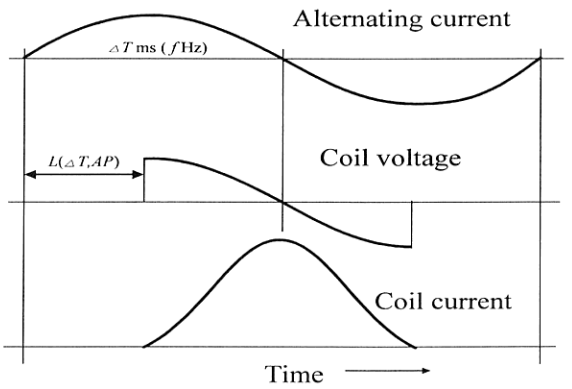

Fig. 8 Outline of current and voltage cycles in FAC

3.4 Measurement part of the gap amplitude

The G_{amp}, which is the measured variable, is measured by the acceleration sensor because of its low sensitivity to environmental changes and the ease of maintenance. The acceleration sensor is installed with metal fittings in the trough fixing part of the experimental feeder. To obtain a standard value of gap measurement, the optical displacement sensor is installed in the experimental feeder. However, the displacement signal with optical sensor is not used for the feedback control for examining of the measuring accuracy of the acceleration sensor signal.

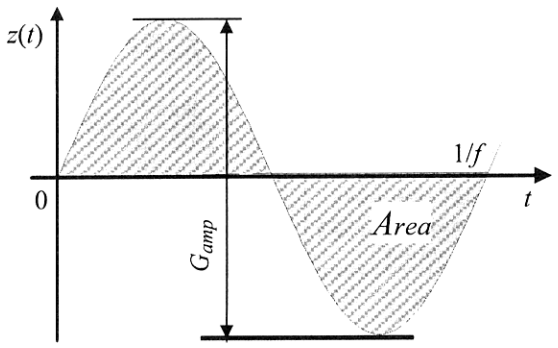

Fig. 9 Scheme for amplitude measurement

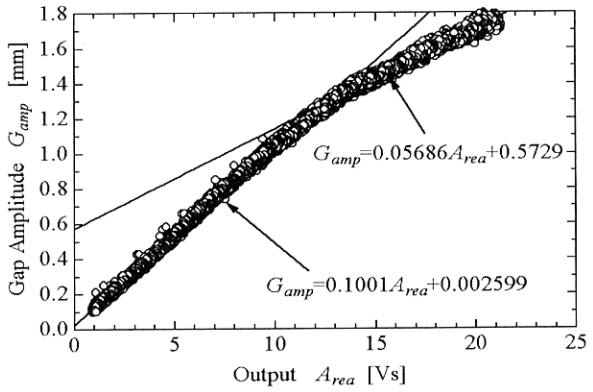

Fig. 10 Relationship between A_{rea} by accelerometer and G_{amp} by opticalsensor

3.4.1 Conversion from the acceleration to the gap amplitude Because the feeder is driven by the firing angle control, an output signal $a(t)$ of the acceleration sensor can be assumed to be a sine wave of amplitudes A and resonance frequency $\omega=2\pi f$ [rad/s].

$$a(t)=A\sin\omega t$$

From this assumption, a gap $z(t)$ is obtained by integrating the acceleration $a(t)$ twice. Therefore, the gap is expressed by the trough displacement and the geometrical relationship of the feeder as follows:

$$z(t)=-\frac{A}{\omega^2}\cos\alpha\sin\omega t=Ka(t). \qquad (5)$$

In other words, gap $z(t)$ is obtained not by integrating the output signal $a(t)$ twice but by multiplying the output signal by the constant because it can be assumed that a wave of the output signal is a sine wave.

The method of obtaining G_{amp} from the gap $z(t)$ is also devised. When the G_{amp} is obtained from the maximum and minimum values of gap $z(t)$ by Eq. (5), it is possible to receive the influence caused by noise directly.

First, area A_{rea} in the hatched part in Fig. 9 is calculated from the output signal $a(t)$ using a acceleration sensor. Next, G_{amp} is obtained based on the A_{rea}. The A_{rea} becomes $A_{rea}=2KA/\omega$ if the output signal is assumed to be a sine wave, and G_{amp} becomes as follows:

$$G_{amp}=2KA=\omega A_{rea}.$$

Therefore, the G_{amp} can be measured by calculating the A_{rea} from the acceleration $a(t)$.

The A_{rea} is calculated by the following steps: (i) To enable a sine wave to be centered at 0 V, an offset (−1.397 V) is removed. (ii) An absoluted wave is generated from the absolute value of the sine wave in step (i). (iii) A trapezoid rule of integration algorithm is applied to the absolute wave in step (ii) and finally the A_{rea} is calculated. The interval time of the integration is 0.25 msec and the sampling time of the acceleration sensor is also 0.25 msec. The integration time is 25 msec of the resonance period $1/f$, and area A_{rea} is calculated using this period. We consider deriving an expression which converts the A_{rea} [Vs] into the output value of the optical displacement sensor.

Figure 10 shows the relationship between the G_{amp} with an optical sensor and the A_{rea} calculated by an acceleration sensor. The relationship between the A_{rea} and the G_{amp} in Fig. 10 shows that it switches at the boundary of 12.6 Vs. This switching characteristic is thought to be nonlinear[1),2)] due to the set of plate springs. Therefore, the expression of conversion was approximated by two straight lines, which changed at the boundary as follows:

$$\begin{cases} G_{amp}=0.100\,1A_{rea}+0.002\,599 & (A_{rea}<12.65), \\ G_{amp}=0.056\,86A_{rea}+0.572\,9 & (A_{rea}\geq 12.65). \end{cases} \qquad (6)$$

3.4.2 Noise caused by transported objects When solids are transported, the transported objects cause an impact on the trough. Therefore, the acceleration is caused by the impact and the noise appears as the output signal of the acceleration sensor. The frequency of this noise changes when the trough and transportation objects are replaced. However, it was confirmed by the experiment that the frequency was 0.5 kHz or more, even when the replacement was conducted. The noise of 0.5 kHz or more was eliminated by the digital low-pass filter $H[z]$ of the third order and A_{rea} can be calculated with low-pass filter using this preprocess. In our experiment, the following filter was used.

$$H[z]=\frac{0.0317+0.0951z^{-1}+0.0951z^{-2}+0.0317z^{-3}}{1-1.4590z^{-1}+0.9104z^{-2}-0.1978z^{-3}}.$$

Figure 11 shows the responses when the noise is removed using this digital filter from the original acceleration sensor output.

3.4.3 Data-processing in measurement process Figure 12 shows the summary of data-processing in the measurement process. First, the output signal by

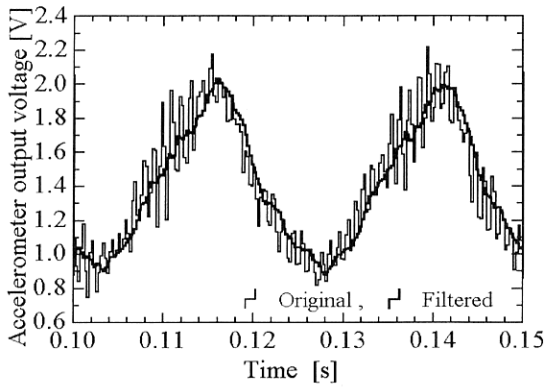

Fig. 11 Effect of a digital low-pass filter

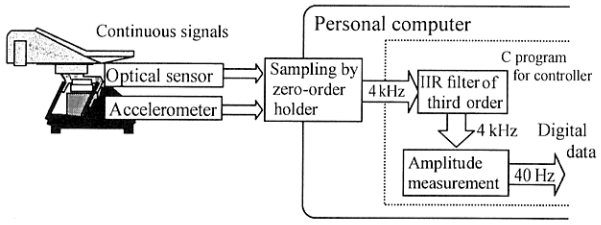

Fig. 12 Signal flow in measurement process

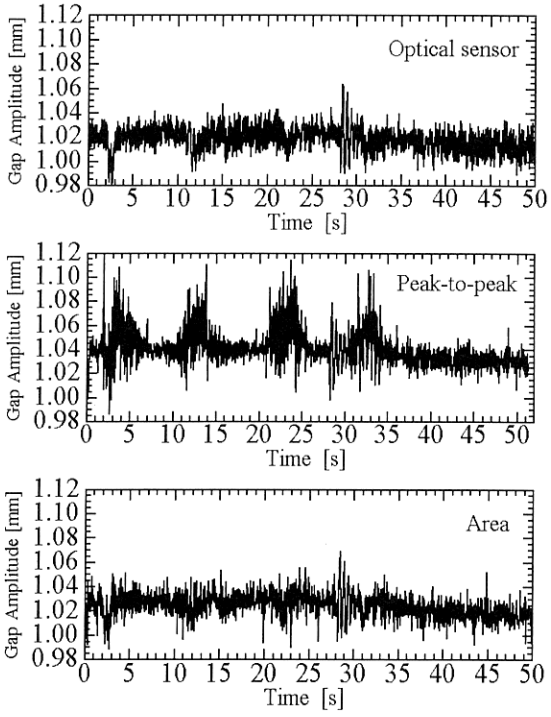

Fig. 13 Performance comparison of sensing methods

the acceleration sensor is sampled at 4 kHz, and the noise is removed by the digital filter. The A_{rea} is calculated from the filtered signal and the G_{amp} is obtained from the relationship of Eq. (6) at the resonance period $1/f$. Figure 13 shows the validity of the G_{amp} obtained by this data-processing, which installed a standard trough by the FAC at AP of 68. Test pieces of 50 g (Wooden column piece of about 0.5 g mass; 8 mm in diameter; 15 mm in length.) were dropped on the trough four times during the driving test. The measurements using an optical sensor and those obtained from of A_{rea}, which was calculated after removing noises, gave similar outputs. However, the noises caused by test pieces appear in the measurement results of the middle figure where the G_{amp} was obtained from the maximum and minimum values at one period. Thus, it is confirmed that the displacement obtained by the acceleration sensor and shows a similar measurement performance as an optical sensor. The effectiveness of this data-processing method to obtain G_{amp} from A_{rea} is confirmed by this result.

3.5 Control part

The structure of the controller is similar to a two-degrees-of-freedom PID controller. The PID controller (hereafter, called the 'feedback controller') takes charge of the disturbance cancellation and the command variable filter takes charge of the improvement in tracking characteristic to the command variable. The command variable filter is indicated by the block of 'transform reference AP' into in shown Fig. 5.

3.5.1 Feedback controller The function of digital feedback controller can be given as follows:

$$u_{FB}[m\Delta t]=K_P\left\{e[m\Delta t]+\frac{\Delta t}{T_I}\sum_{k=0}^{m}e[k\Delta t]+\frac{T_D}{\Delta t}(e[m\Delta t]-e[(m-1)\Delta t])\right\}, \quad (7)$$

where e is the error, Δt is the sampling time, K_P is proportional gain, T_I is integration time and T_D is differentiation time. In the control experiment, rough values of these parameters were obtained by the ultimate sensitivity method[5], assuming $K_P=12.0$, $T_I=0.10$, and $T_D=0.25$ by adjustment.

3.5.2 Command variable filter The command variable filter calculates the steady-state amplitude power AP_{eqn} based on the command variable. The derivative controller for tracking the reference (command) in Fig. 5 works to improve the tracking characteristic to the command variable. In this study, we apply a nonlinear function $f(r)$ to the command variable filter, though a proportional controller is generally used as a command variable filter. The stability of the system is not problem because this nonlinear element gives a unique output by the command variable. This nonlinear element is also independent of the feedback system. Figure 14 shows the relationship between the command variable and the AP obtained by an experiment using a standard trough. The command variable filter was obtained based on these results, as follows:

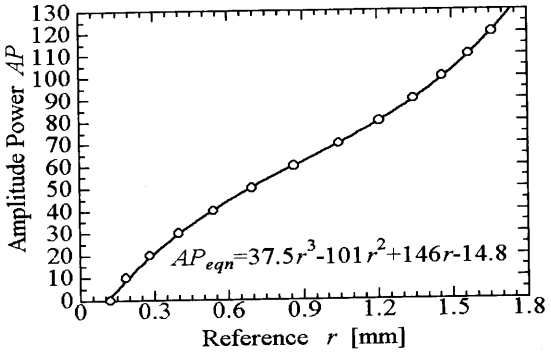

Fig. 14 Relationship between r and AP

$$AP_{eqn}=f(r)$$
$$=37.5r^3-101r^2+146r-14.8. \quad (8)$$

The derivative controller, which improved the tracking performance to the command variable, was assumed to be an approximate differentiation according to the first-order transfer function as follows:

$$D_{FF}(s)=\frac{\gamma s}{\beta s+1} \quad (9)$$

This derivative controller and the command variable filter (8) are obtained in discrete-time realization at sampling time Δt, and the command variable filter $u_{FF}[m\Delta t]$ is obtained as follows:

$$u_{FF}[m\Delta t]=f(r[m\Delta t])-\gamma\{\beta_1(r[m\Delta t]-r[(m-1)\Delta t])-\beta_2 u_{FF}[(m-1)\Delta t]\},$$

where β_1 and β_2 are necessary for the discrete counterpart of coefficients as follows:

$$\beta_1=\beta^{-1},\ \beta_2=-\exp(-\Delta t\beta_1).$$

Parameters $\gamma=6.0$ and $\beta=0.1$ were used for the control experiment.

4. Control Experiment for a Standard Trough

4.1 Change in mass of transportation objects

The performance in disturbance cancellation when the mass of the transportation objects changes is verified by the experiment for a standard trough.

Figure 15 shows the time behavior when the command variable of the G_{amp} is assumed to be 0.2 mm, and test pieces of 200 g are dropped in an empty trough. The short dashed line indicates the FAC, and the solid line indicates the feedback control. Using the FAC, the G_{amp} recovers after decreasing, when the transported objects are dropped off (test pieces fall from the trough by transportation and the mass of test pieces on the trough decreases). On the other hand, with the feedback control, the G_{amp} recovers in about 8 sec after the test pieces are dropped on the trough.

Thus, the feedback control can cancel the disturbance which increases the mass of transportation objects suddenly.

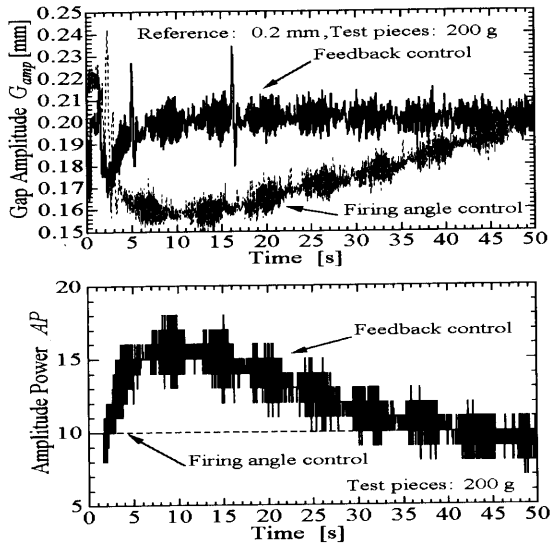

Fig. 15 Effect of transporting wooden plugs

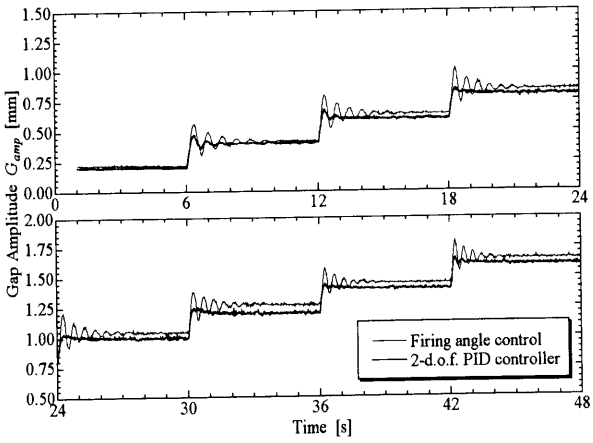

Fig. 16 Stepresponses with 2-d.o.f. controller

4.2 Tracking characteristic to command variable

The improvement of the tracking characteristic to the command variable is confirmed using a standard trough by an experimental step response. Figure 16 shows the experimental results. The short dashed line indicates the response using the FAC, and the solid line shows the response using the feedback control. A response with vibration and steady-state deviation was observed with the FAC when the command variables increased. On the other hand, the response with feedback control shows improved tracking characteristic and no steady-state deviation. In particular, the response with feedback control G_{amp} in of 1.0 mm shows an excellent tracking response because the PID parameters are adjusted in the G_{amp} of 1.0 mm. However, the characteristic of feeder changes depends on the G_{amp}. Therefore, the response when the G_{amp} has an other value is worse than the

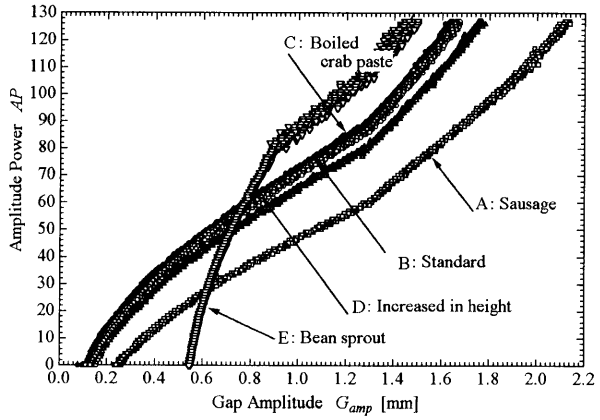

Fig. 17 Relationship between G_{amp} and AP

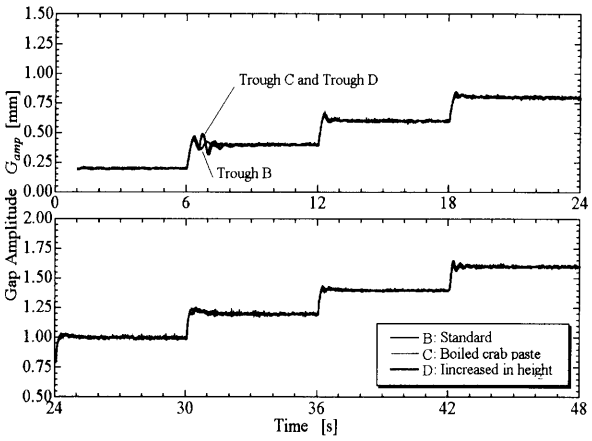

Fig. 18 Step responses of group G

response in case G_{amp} of of 1.0 mm.

5. Control Experiment with Different Troughs

5.1 Grouping of troughs

It has already been mentioned that the types of troughs exceed 100. Therefore, adjusting the PID parameters for an individual trough increasses costs. Hence, we consider a method which can control several kinds of troughs using the same PID parameters. In this study, we consider a method in which we adjust the command variable filter based on experimental results for five kinds of troughs mentioned in Table 2.

The relationship between AP and G_{amp} is shown in Fig. 17 for five kinds of troughs (in Table 2). We performed the following automatic experiment: (i) The feeder is driven by increasing AP every 0.2 sec from 0 to 127, and decreasing every 0.2 sec from 127 to 0. (ii) During this driving, AP and G_{amp} are measured automatically. The results of this automatic experiment were plotted in Fig. 17. The time taken for this experiment was about 50 sec because this relationship can be obtained for several kinds of troughs easily.

Figure 17 shows that troughs C, D and the standard trough B have similar relationships. Trough A, which is light, vibrates well compared to other troughs and the range of amplitude is also wide. On the other hand, trough E, which is heavy, requires more AP and the range of amplitude is narrow. From these results, troughs of shapes and parameters can be grouped together based on the relationship between AP and G_{amp}.

5.2 Tracking characteristic to command variable for trough group

Troughs B, C, and D having similar relationships between AP and G_{amp} are grouped as trough group G. We performed experiments on feedback control on trough group G using the same PID parameters of the feedback controller. Figure 18 shows the experimental step response.

The output responses of troughs B, C and D correspond considerably, as shown in Fig.18, therefore, the relationships between AP and G_{amp} is similar for the group. Therefore, it is possible to control using the same PID parameters and the same command variable filter. From the results we consider that the same PID parameters and the same command variable filter can be used to control the system if the relationship between AP and G_{amp} are similar. Thus, the number of controllers and the time required for PID parameter adjustment could be decreased if we group the troughs taking into account the relationship between AP and G_{amp}.

5.3 Adjustment of the command variable filter

It is confirmed that tracking characteristic to the command variable can be improved by adjusting the command variable filter.

In our experiment, the command variable filter (8) based on a standard trough is called 'standard filter.' Moreover, the command variable filter which adjusts individually based on the relationship between AP and G_{amp} for trough E is called 'individually adjusted filter' and can be expressed as follows:

$$AP_{equ}=\bar{f}(r)$$
$$=264r^3-906r^2+1100r-370 \quad (11)$$

Figure 19 shows the step responses using a standard filter and an individually adjusted filter. When the command variables are 0.65 mm, 0.75 mm, 0.85 mm and 0.95 mm, the transient responses are different with respect to the difference of the command variable filter. The response is ineffective if a standard filter is used, however, it is improved with individually adjusted filters though the response vibrate. When the command variable is 0.95 mm or more, an excellent tracking characteristic is shown regardless of the individually adjusted filter. We consider that the reason is the integral gain of feedback controller

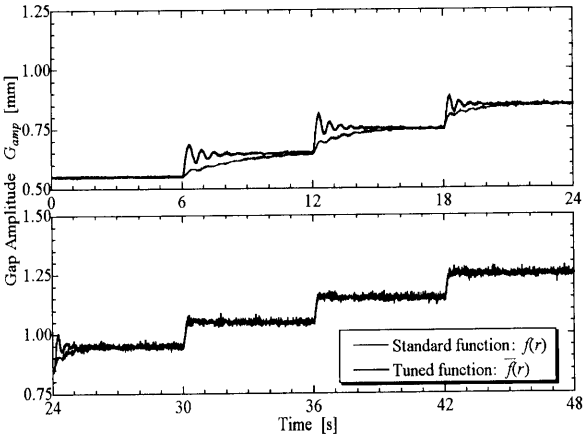

Fig. 19 Comparison of step responses by $f(r)$ and those by $\bar{f}(r)$

because the difference in the relationship shows a few offsets in the range where G_{amp} is larger than 0.9 mm as shown in Fig. 17.

When grouping is difficult because the relationship between AP and G_{amp} is considerably different, an adjustment of the command variable filter is effective. Therefore, it is thought that the tracking characteristic to the command variable is improved if the command variable filter is adjusted for trough A.

6. Conclusions

In this study, we have reported our attempts and experiments on the feedback control of feeders. The conclusions are summarized as follows.

(1) A structure of two-degrees-of-freedom PID control system containing the FAC driver was proposed.

(2) The control performance with the proposed feedback control system and that with the FAC were compared.

(3) We confirmed through experiments that the trough group for which the relationship between AP and G_{amp} are similar can be controlled using the same PID parameters and the same command variable filter.

(4) We confirmed through experiments that the adjustment of the command variable filter is effective when the relationship between AP and G_{amp} shows a considerable difference.

References

(1) Konishi, S., Sakaguchi, K., Amijima, S., Matsuoka, T., Okano, I. and Morinaka, H., Non-Linear Phenomenon Observed on Resonance Curve for Vibratory Feeder-Electromagnetic Type, Proc. APVC '95, (1995), pp. 258-263.

(2) Konishi, S., Sakaguchi, K., Amijima, S., Matsuoka, T., Okano, I. and Morinaka, H., Analysis of Non-Linear Resonance Phenomenon for Vibratory Feeder, Proc. APVC '97, (1997), pp. 854-859.

(3) The Institute of Electrical Engineers of Japan (ed.), Magnetic Levitation and Magnetic Bearing, (in Japanese), (1993), p. 30, Corona Publishing Co., Ltd.

(4) Doi, T., Yoshida, K., Tamai, Y., Kono, K., Naito, K. and Ono, T., Feedback Control for the Vibratory Feeder of Electromagnetic Type, Proc. ICAM '98, (1998), pp. 849-854.

(5) Suda, N., PID control, (in Japanese), (1992), Asakura Publishing Co., Ltd.

(6) Araki, M. and Taguchi, H., Two-Degrees-of-Freedom PID Controller, Journal of the Institute of Systems, Control and Information, Vol. 42, No. 1 (1998), pp. 18-25.